

Cytoplasmic LEK1 is a regulator of microtubule function through its interaction with the LIS1 pathway

Victor Soukoulis*, Samyukta Reddy*, Ryan D. Pooley*, Yuanyi Feng†, Christopher A. Walsh†, and David M. Bader**

*Stahlman Cardiovascular Research Laboratories, Program for Developmental Biology, and Department of Medicine, Vanderbilt University Medical Center, Nashville, TN 37232-6300; and †Howard Hughes Medical Institute, Beth Israel Deaconess Medical Center, and Department of Neurology, Harvard Medical School, Boston, MA 02115

Edited by Eric N. Olson, University of Texas Southwestern Medical Center, Dallas, TX, and approved May 5, 2005 (received for review March 21, 2005)

LIS1 and nuclear distribution gene E (NudE) are partner proteins in a conserved pathway regulating the function of dynein and microtubules. Here, we present data that cytoplasmic LEK1 (cytLEK1), a large protein containing a spectrin repeat and multiple leucine zippers, is a component of this pathway through its direct interaction with NudE, as determined by a yeast two-hybrid screen. We identified the binding domains in each molecule, and coimmunoprecipitation and colocalization studies confirmed the specificity of the interaction between cytLEK1 and NudE. Confocal deconvolution analysis revealed that cytLEK1 exhibits colocalization with endogenous NudE and with the known NudE binding partners, LIS1 and dynein. By localizing the NudE-binding domain of cytLEK1 to a small domain within the molecule, we were able to disrupt cytLEK1 function by using a dominant negative approach in addition to LEK1 knockdown and, thus, examine the role of the cytLEK1–NudE interaction in cells. Consistent with a defect in the LIS1 pathway, disruption of cytLEK1 function resulted in alteration of microtubule organization and cellular shape. The microtubule network of cells became tightly focused around the nucleus and resulted in a rounded cell shape. Additionally, cells exhibited a severe inability to repolymerize their microtubule networks after nocodazole challenge. Taken together, our studies revealed that cytLEK1 is essential for cellular functions regulated by the LIS1 pathway.

cytoskeleton

The microtubule network plays a critical role in a range of functions, including mitosis, organelle positioning, cell shape, and migration (1–3). However, the precise regulation of microtubule and dynein function remains poorly understood, despite knowledge of their interaction with several important partner proteins. One such partner is LIS1, a microtubule-associated protein that, when mutated, results in lissencephaly, a brain malformation caused by defective migration and proliferation of neuronal precursors (4, 5). LIS1 regulates microtubule dynamics through its association with dynein (6, 7). However, the exact role of LIS1 remains poorly defined, especially with regard to the required partners that regulate function. Nuclear distribution element (NudE) and its isoform Nudel bind to LIS1 and dynein and play similar roles in LIS1 regulation of dynein (8–11). We use the term NudE-like [NudE(L)] to describe both proteins. Inhibition of NudE(L) function by using various dominant negative proteins disrupts CNS architecture in *Xenopus*, microtubule network organization, dynein localization, and spindle formation (8, 10, 12). NudE(L) also regulates dynein-directed transport along the mitotic spindle and influences membrane traffic, in association with LIS1 (11, 13).

Regulation of the LIS1 pathway is a complex process. Identical phenotypes are not observed with regard to the cytoskeleton and distribution of key proteins, for example, from disruption of pathway components (6, 8–10, 13, 14). Additionally, LIS1, NudE(L), and dynein have significant but not completely overlapping distributions within cells, and individual components of this pathway, such as NudE, have dynamic subcellular distributions and expres-

sion patterns (6, 8, 10, 15). Thus, although the importance of the LIS1 pathway and its regulation of the cytoskeleton are well established, the complexity and potential for interaction of this pathway with additional protein networks are just emerging.

Our laboratory has studied the structure, expression, and function of LEK1, a relatively large murine protein (>300 kDa) highly related to CMF1 (chicken) and CENP-F/mitosin (human) (16, 17). These proteins share a similar domain structure comprised of a cluster of leucine zippers in the N terminus, a central spectrin repeat, and a nuclear localization sequence along with an atypical retinoblastoma-binding domain in the C terminus (18–20). Despite their homology, the members of this family exhibit variable expression patterns and functions. LEK1 is unique in that it is posttranslationally cleaved to yield two peptide products: an N-terminal cytoplasmic LEK1 (cytLEK1), which has a cytoplasmic distribution, and a shorter C-terminal nuclear LEK1 present in the nucleus.

Until now, studies have focused on the role of C-terminal domains in the members of the LEK1/CMF1/CENP-F family (17, 20–22). The C terminus of CENP-F is critical for its dimerization ability and mitotic function (23). Similarly, nuclear LEK1, which contains the retinoblastoma (Rb)-binding domain, binds to the “pocket” region of all Rb family members and thus potentially influences their activity (24). LEK1 depletion results in arrest of proliferation consistent with activation of Rb family member function. With the focus of studies on C-terminal domains, the N-terminal and central regions have not been carefully examined. Thus, little if anything is known about the function of the larger protein, cytLEK1, and what processes it may regulate. Importantly, the presence of a spectrin repeat, which may serve as a cytoskeletal and signal transduction docking region (25), and numerous leucine zippers, which participate in protein–protein interactions (26), suggested a possible cytoskeletal role for cytLEK1.

In an effort to elucidate cytLEK1 function, we conducted a yeast two-hybrid screen by using the spectrin repeat region of cytLEK1 as bait. The major binding partner identified in this assay was NudE. This interaction supported our hypothesis of a cytoskeletal role for cytLEK1 through the spectrin repeat. Additionally, NudE(L) and LIS1 are highly expressed in the developing heart, skeletal muscle, and brain, similar to LEK1 (8, 11, 15, 20, 27). Here, we characterize this cytLEK1–NudE interaction and reveal colocalization of cytLEK1 with several LIS1 pathway members. Notably, disruption of cytLEK1 function by using multiple experimental approaches reveals severe effects on the cytoskeleton and cell morphology, consistent with the role of cytLEK1 as a regulator of the LIS1 pathway.

Materials and Methods

Immunocytochemistry and Microscopy. Cells grown on glass chamber slides were washed with PBS before fixation and extraction. Primary

This paper was submitted directly (Track II) to the PNAS office.

Abbreviations: SRR, spectrin repeat region; NudE, nuclear distribution gene E; NudE(L), NudE and NudE-like; cytLEK1, cytoplasmic LEK1.

†To whom correspondence should be addressed at: Stahlman Cardiovascular Laboratories, Program for Developmental Biology, Department of Medicine, 346 PRB, Vanderbilt University Medical Center, Nashville, TN 37232-6300. E-mail: david.bader@vanderbilt.edu.

© 2005 by The National Academy of Sciences of the USA

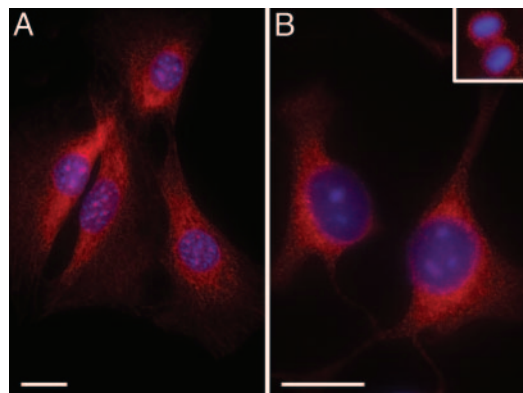


Fig. 1. Distribution of cytLEK1 in murine cell lines. CytLEK1 is distributed widely in the cytoplasm of 3T3 fibroblasts (A) and C2C12 myoblasts (B). The protein is concentrated more highly around the nucleus. (Inset) In mitotic cells, cytLEK1 is mostly excluded from regions containing DNA. DAPI (blue) was used to visualize nuclei. Intense nuclear puncta are secondary antibody artifacts. (Bars: 10 μ m.)

and secondary antibodies were applied, and cells were visualized by fluorescence microscopy on an AX70 (Olympus, Melville, NY) or, for confocal analysis, an LSM510 (Zeiss) microscope. Deconvolution analysis was performed on confocal Z stacks (0.5- μ m optical thickness) by using a blind 3D deconvolution algorithm (AutoQuant Imaging, Troy, NY).

Yeast Two-Hybrid Screen and Characterization of Interactions. The spectrin repeat region of cytLEK1 (amino acids 1,906–2,149) was PCR-amplified from a full-length cytLEK1 vector (amino acids 1–2,210) and cloned into pGBKT7 to be used as bait in a Matchmaker Y2H System 3 screen (Clontech). The bait was mated with yeast pretransformed with a whole-mouse embryonic-day-11 cDNA library. Yeast colonies that survived on quadruple dropout medium and exhibited a blue color upon Gal testing were subjected to further evaluation. Resulting sequences from library plasmids were identified by National Center for Biotechnology Information BLAST (28). False positive tests involving empty vector and an unrelated protein were conducted to eliminate spurious interactions per the manufacturer's instructions.

The cytLEK1 spectrin repeat region (SRR) and NudE yeast deletion constructs were created by using a PCR approach and transformed into AH109 and Y187 yeast, respectively, for matings. Deletion constructs were created as shown in Fig. 2A. Colonies were grown on quadruple dropout medium and tested for Gal expression to determine viable interactions. To confirm results by coimmunoprecipitation in mammalian cells, the relevant cytLEK1 plasmid insert was cloned into the pCMV-myc mammalian expression vector (Clontech). Additionally, GFP-mNudE (8) was used for transfection studies.

COS-7 cells grown on 10-cm plates were harvested 48 h after transfection for use with the ProFound mammalian c-Myc tag coimmunoprecipitation kit (Pierce) according to the manufacturer's protocol. Eluted protein was subject to SDS/PAGE analysis followed by immunoblotting. Lysate (10 μ g per lane) was used to confirm protein expression. Blots were developed by using nitroblue tetrazolium/5-bromo-4-chloro-3-indolyl phosphate (Roche) and scanned into digital format (Hewlett-Packard).

Nocodazole Treatment. Cells were transfected with the appropriate plasmid and exposed to nocodazole (Sigma), a microtubule depolymerizing agent, at a final concentration of 5 μ g/ml for 3 h in the appropriate serum conditions. After washing out the drug three times with medium, the cells were grown for 0, 10, or 20 min before preextraction (for myc-C) and fixation.

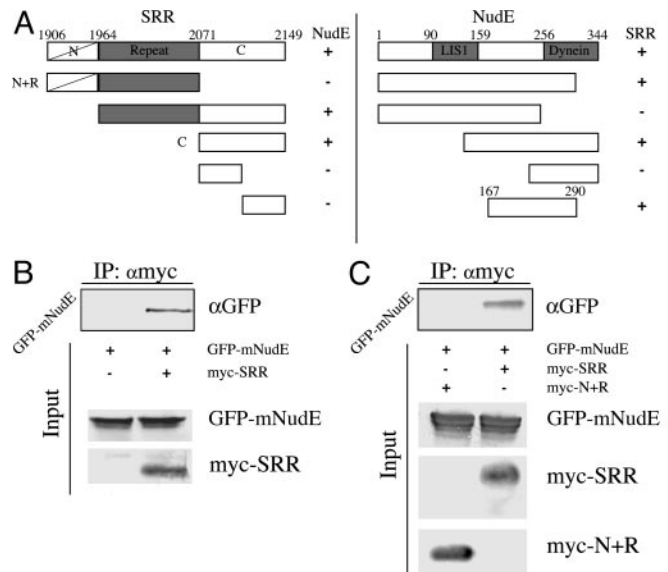


Fig. 2. Examination of cytLEK1-NudE interaction and identification of binding domains. (A) Deletion constructs of SRR were tested for interaction with full-length NudE in a yeast two-hybrid assay. +, Matings that grew on quadruple dropout medium. The C domain (amino acids 2071–2149) is required and sufficient for interaction with NudE. Similarly, deletion constructs of NudE were assembled. The LIS1- and dynein-binding domains of NudE(L) are shown. The SRR and C domain of cytLEK1 bind to amino acids 167–290 of NudE. (B) COS-7 cells were transfected with GFP-mNudE alone or GFP-mNudE and myc-SRR. Lysates were immunoprecipitated with an anti-myc antibody, and blots were probed with anti-GFP. Protein expression was confirmed by blotting lysate lanes. GFP-mNudE is coimmunoprecipitated with myc-SRR when coexpressed but not in the absence of myc-SRR. (C) When COS-7 cells are cotransfected with GFP-NudE and myc-N+R, GFP-mNudE is not detected in the precipitant. Thus, the C domain is required for the interaction between cytLEK1 and NudE.

Morpholino Antisense Oligomer Treatment. Morpholinos specific to the 5' UTR of the *LEK1* mRNA were constructed, tested, and applied as described in ref. 24. Standard control morpholinos were provided by the manufacturer (Gene Tools, Carvalis, OR). Cells were treated per the manufacturer's instructions. Seventy-two hours after treatment, cells were prepared for microscopic examination as described above. When confirming cytLEK1 knockdown, special attention was taken to ensure that all antibody concentrations, camera exposure times, and PHOTOSHOP (Adobe Systems, San Jose, CA) preparations were identical and conducted in parallel.

Supporting Information. Details are provided in *Supporting Materials and Methods* and Figs. 8–11, which are published as supporting information on the PNAS web site.

Results

Subcellular Distribution of cytLEK1 and Identification of Interacting Proteins. Analysis of 3T3 fibroblasts and C2C12 myoblasts reveals a predominantly cytoplasmic distribution pattern for cytLEK1 (Fig. 1). Additionally, cytLEK1 localizes more intensely to a perinuclear location in cells. During mitosis, cytLEK1, like nuclear LEK1 (20), is mostly excluded from regions containing DNA (Fig. 1B Inset).

To identify cytLEK1 binding partners, a yeast two-hybrid approach was undertaken by using the SRR (amino acids 1906–2149) as bait. Two screens yielded 117 and 94 clones, and, of these, 12 and 19 clones, respectively, were found to be full-length NudE. After false positive screening, NudE represented the majority of remaining clones that displayed a specific interaction with the SRR. Given the known expression pattern and cytoskeletal function of NudE, its putative interaction with cytLEK1 was pursued.

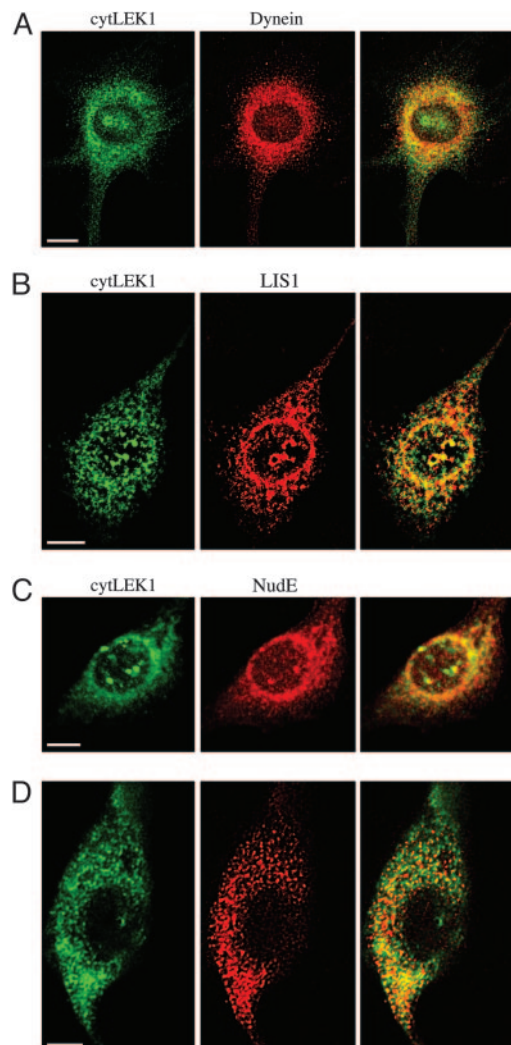


Fig. 3. CytLEK1 colocalizes with members of the LIS1 pathway in murine cells. Colocalization of endogenous proteins in 3T3 fibroblasts was examined by confocal microscopy. (*A*, *B*, and *D*) Deconvolution analysis (0.5- μm optical sections) was additionally conducted for the highest level of detail. CytLEK1 is in green. (*A*) CytLEK1 and dynein (red) colocalize significantly near the nucleus. (*B*) CytLEK1 also colocalizes with LIS1 (red) in this perinuclear region. (*C* and *D*) CytLEK1 and NudE (red) colocalize extensively near the nucleus but less at the cell periphery. Intense nuclear puncta are secondary antibody artifacts. (Bars: 5 μm .)

Identification of the Binding Domains of cytLEK1 and NudE. Yeast two-hybrid techniques were used to determine which region within the SRR of cytLEK1 interacted with NudE by dividing the SRR into the N domain (amino acids 1906–1964), the repeat (R) domain (amino acids 1964–2071), and the C domain (amino acids 2071–2149). Only those constructs containing the C domain, not necessarily the R domain itself, retained interaction with full-length NudE (Fig. 2*A*). In fact, the C domain alone was sufficient for interaction and further truncation eliminated all binding, suggesting that amino acids 2071–2149 of cytLEK1 are critical for interaction with NudE. No other proteins were detected during screening that were capable of specifically interacting with the C domain alone. Similar deletion studies with NudE revealed that a C-terminal region of NudE (amino acids 167–290) was required and sufficient for the interaction with the C domain of cytLEK1 (Fig. 2*A*). Interestingly, this region in NudE(L) overlaps its known dynein-binding domain (10, 13).

To determine whether cytLEK1 and NudE interact in mammalian cells, similar myc-tagged deletion constructs were con-

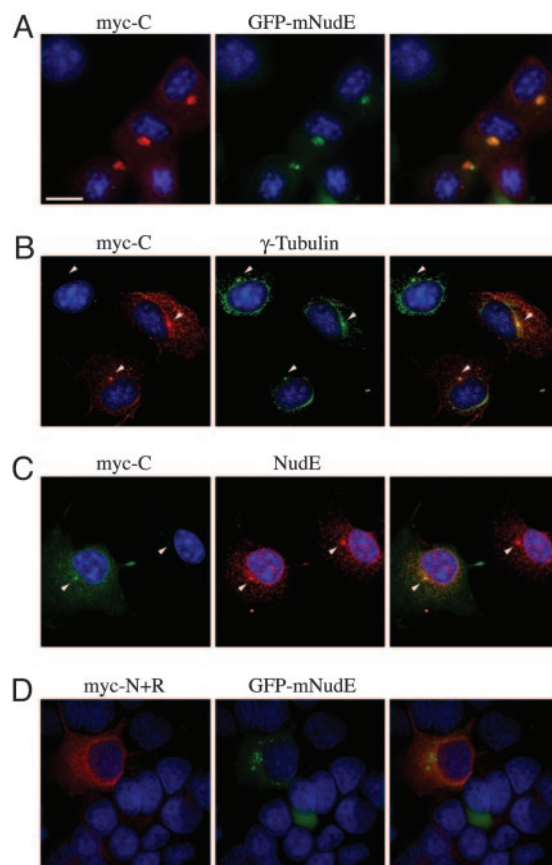


Fig. 4. Myc-C colocalizes with NudE and γ -tubulin in COS-7 cells. (*A* and *D*) GFP-mNudE is in green and myc-tagged proteins are in red. (*B* and *C*) Arrowheads mark the γ -tubulin and NudE centrosomal spots. (*A*) COS-7 cells were cotransfected with myc-C and GFP-mNudE and examined after 24 h. The merged image shows clear colocalization of these two proteins at a distinct cellular spot. (*B*) Myc-C (red) colocalizes with endogenous γ -tubulin (green) at the centrosome. (*C*) Myc-C (green) also colocalizes with endogenous NudE (red) present at the centrosome. (*D*) Myc-N+R, which lacks the NudE-binding domain, does not colocalize with GFP-mNudE. DAPI (blue) was used to visualize nuclei. (Bar: 10 μm .)

structed. COS-7 cells were cotransfected with myc-SRR and GFP-mNudE for coimmunoprecipitation analysis. GFP-mNudE coimmunoprecipitates with myc-SRR, confirming the two-hybrid data and demonstrating the interaction between cytLEK1 and NudE (Fig. 2*B*). Importantly, GFP-mNudE is unable to be coimmunoprecipitated with myc-N+R, which lacks the C domain (Fig. 2*C*). Therefore, the C domain is indeed required for the binding of cytLEK1 and NudE. Taken together, these results demonstrate the interaction of cytLEK1 and NudE in mammalian cells and map this interaction to specific domains in both proteins.

cytLEK1 Colocalizes with NudE and NudE-Binding Partners in Murine Cells.

We next examined the endogenous localization of cytLEK1 relative to NudE and other LIS1 pathway members by using confocal deconvolution analysis. CytLEK1 displays significant colocalization with dynein in both 3T3 and C2C12 cells with the greatest overlap in perinuclear regions (Fig. 3*A*). The perinuclear staining is not an artifact of high protein concentrations in these areas, as colabeling of cytLEK1 with markers for myosin, actin, desmin, or vimentin does not reveal any noticeable colocalization (see Figs. 9 and 10). Our results revealed that the colocalization of cytLEK1 and dynein is not absolute. Although there is substantial colocalization near the nucleus, it becomes less apparent toward the periphery of cells, consistent with previous confocal studies of LIS1 pathway members (6, 29). Indeed, LIS1 does not colocalize com-

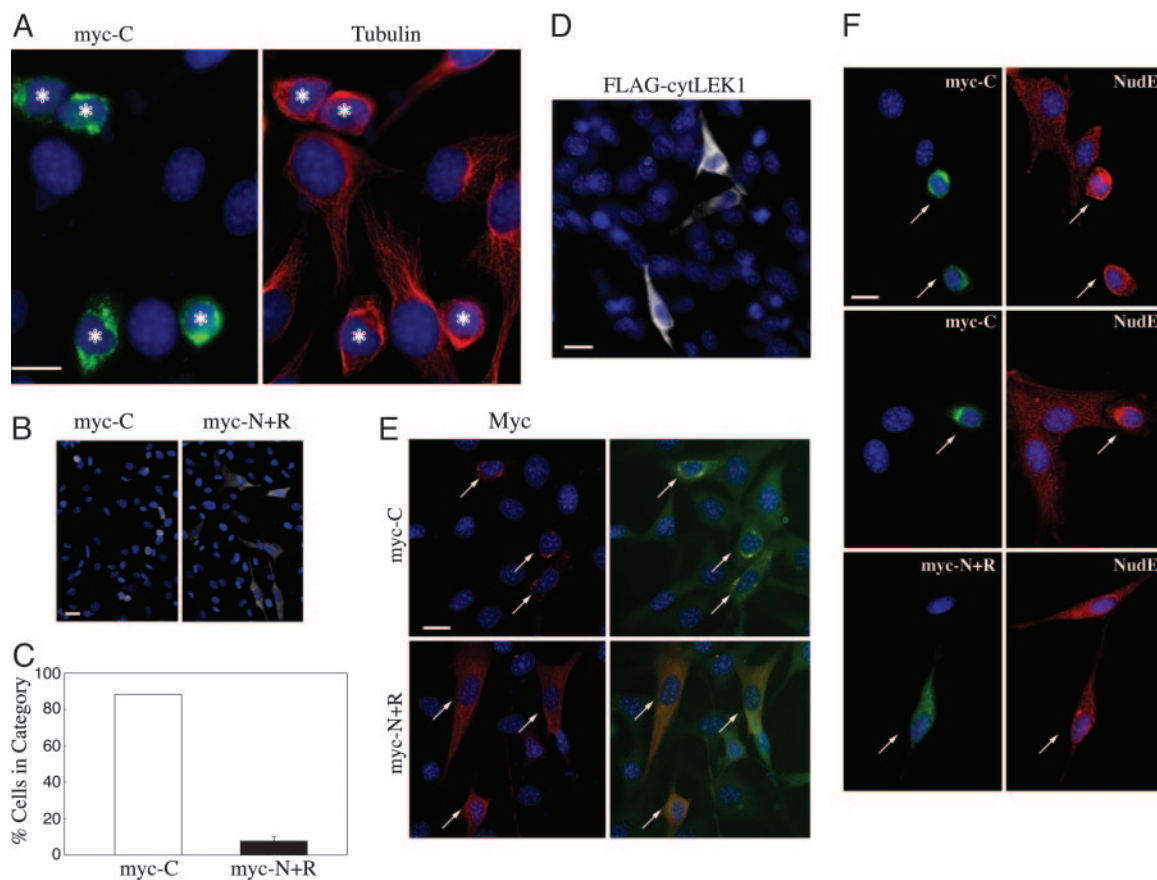


Fig. 5. Disrupting cytLEK1 function alters microtubule network organization and cell shape. (A–C) 3T3 cells were transfected with myc-C or myc-N+R and examined for cytoskeletal and morphological changes after 24 h. (B and D) Fluorescence of transfected cells was converted to grayscale. (A) Cells expressing myc-C (green; asterisks) have an altered microtubule network (red) and rounded morphology. The network is tightly focused around the nucleus. (B) The majority of cells expressing myc-C exhibit this phenotype, unlike myc-N+R-expressing cells. (C) When quantified, 88% of myc-C-expressing cells are affected versus 7.7% of myc-N+R-expressing cells, a statistically significant difference ($P < 0.0001$ by Mann–Whitney U test; PRISM 3.0, GraphPad, San Diego). (D) C2C12 cells transfected with a construct of intact cytLEK1 do not exhibit any such changes. (E) 3T3 cells were transfected with myc-C or myc-N+R (red; arrows), and any nonrounded cells, which were a small minority of the total myc-C population, were examined. The myc-C protein is distributed in a perinuclear fashion in these cells, whereas the myc-N+R protein shows no such specific localization (phalloidin is green). (F) Endogenous NudE distribution (red) is altered in 3T3 cells expressing myc-C but not myc-N+R (both green; arrows). This perinuclear accumulation of NudE is evident in all cells regardless of morphology. DAPI (blue) was used to visualize nuclei. (Bars: A and D–F, 10 μm ; B, 20 μm .)

pletely with dynein, especially near the cell periphery. Deconvolution analysis similarly demonstrated a high degree of colocalization between cytLEK1 and LIS1, especially in perinuclear regions. (Fig. 3B). Examination of NudE localization in 3T3 cells revealed a perinuclear distribution, consistent with Nudel in this cell type (9, 10, 30). Our results confirm that NudE also is present at more than just the centrosome. CytLEK1 and NudE exhibited a similar distribution in our confocal studies (Fig. 3C). Deconvolution analysis of confocal images (Fig. 3D) further defined the highest amount of colocalization to be near the nucleus, as described above for the two other LIS1 pathway members.

myc-C Colocalizes with NudE and γ -Tubulin in COS-7 Cells. We also examined whether the C domain alone can direct this colocalization of cytLEK1 and NudE (Figs. 4 and 8). Initially, COS-7 cells were cotransfected with myc-SRR or myc-C and GFP-mNudE. Myc-SRR and GFP-mNudE exhibited extensive overlap in staining, predominantly at the centrosome (8). Importantly, expression of the C domain alone directs this colocalization at the centrosome in COS-7 and 3T3 fibroblasts (Fig. 4A), as confirmed by endogenous γ -tubulin staining (Fig. 4B). Additionally, myc-C colocalizes with endogenous NudE protein present at the centrosome and perinuclear region (Fig. 4C), reiterating the specificity of the C domain for binding to NudE. Confirming the critical importance of the C

domain for NudE colocalization, myc-N+R does not colocalize with GFP-mNudE in COS-7 cells (Fig. 4D).

Disrupting cytLEK1 Function Alters Cell Shape and Microtubule Network Organization. Alterations in LIS1 pathway function cause abrupt changes in the microtubule network and cell morphology (6, 8, 14). Because cytLEK1 interacts and colocalizes with key components of the LIS1 pathway, we postulated that inhibition of cytLEK1 function would disrupt cellular processes regulated by these proteins. We tested the ability of the myc-C protein to act in a dominant negative fashion by uncoupling the NudE-binding site in cytLEK1 from other functions in the intact molecule.

Expression of myc-C in 3T3 and C2C12 cells results in a drastic alteration of the cytoskeletal network and cell morphology (Fig. 5). The microtubule network is collapsed around the nucleus and has lost its regular broad cytoplasmic distribution. Additionally, the cells adopt a rounded morphology as soon as 8 h after transfection. This phenotype is consistent with reported dominant negative and knockdown studies of LIS1 pathway members (6, 14, 30, 31). Notably, the cells expressing myc-C do not detach from the plate even after 72 h; thus, this effect is not likely to be a simple cell death response. Conversely, expression of full-length cytLEK1 or myc-N+R, which lacks the NudE-binding domain, does not affect morphology or cytoskeletal organization (Fig. 5B and D), suggest-

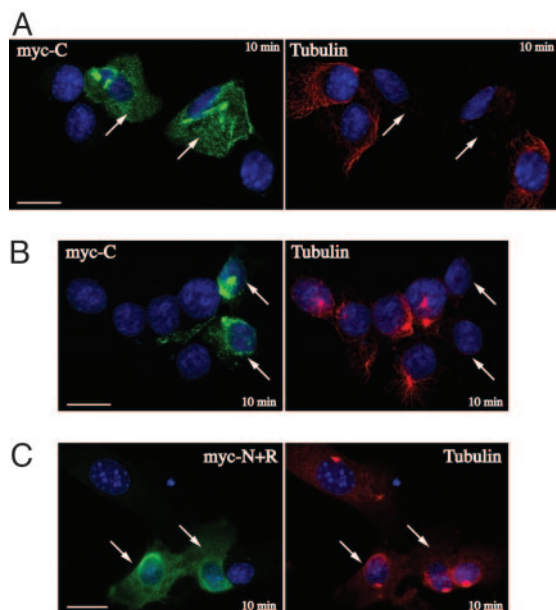


Fig. 6. Disrupting cytLEK1 function inhibits microtubule repolymerization after nocodazole challenge in murine cells. Myc-tagged proteins are in green (arrows), and tubulin is in red. (A and B) Expression of myc-C in C2C12 (A) and 3T3 (B) cells causes a severe inhibition in microtubule repolymerization after nocodazole washout. Microtubule networks are almost completely absent in transfected cells. (C) 3T3 cells transfected with myc-N+R do not show any noticeable inhibition in microtubule repolymerization. DAPI (blue) was used to visualize nuclei. (Bars: 10 μ m.)

ing that this phenotype is specific to isolation of the NudE interaction domain. Cell counts determined that $88 \pm 3\%$ of the myc-C-transfected cells and only $7.7 \pm 2\%$ of the myc-N+R-transfected cells display the aforementioned phenotype after 24 h (Fig. 5C, $P < 0.0001$). Examining the small number of cells initially resistant to myc-C disruption revealed a tight perinuclear localization of this protein, in contrast to the diffuse distribution of myc-N+R (Fig. 5E). Interestingly, an altered distribution of endogenous dynein, LIS1, and NudE is observed in cells expressing myc-C but not myc-N+R (Figs. 5F and Fig. 8). Similar to myc-C, these proteins are highly concentrated near the nucleus. This lack of peripheral distribution is evident even in cells that have not yet undergone a change in morphology (Fig. 5F). Notably, by 72 h after transfection, nearly all cells transfected with myc-C have adopted the perinuclear microtubule network and rounded morphology. The action of myc-C is likely due to its association with the cytoskeleton, because a detergent preextraction protocol (32–34) revealed that the C domain confers detergent resistance. After preextraction, myc-C, unlike myc-N+R, remained in the insoluble cytoskeletal pool (Fig. 8) and thus may incorporate with the cytoskeleton to mediate the disruptions in LIS1 pathway function described here.

Disrupting cytLEK1 Function Inhibits Microtubule Repolymerization. Expression of myc-C has a strong effect on the organization of the intact microtubule network. Because alteration of LIS1 pathway function disrupts microtubule polymerization and localization after nocodazole treatment (6, 30), we determined whether myc-C expression resulted in a similar phenotype. Remarkably, C2C12 and 3T3 cells expressing myc-C showed a nearly complete and long-lasting inability to repolymerize their microtubule networks after nocodazole washout (Fig. 6A and B). Although the surrounding nontransfected cells have long networks emanating from their organizing centers, transfected cells lack microtubule segment formation. Importantly, expression of myc-N+R, which does not

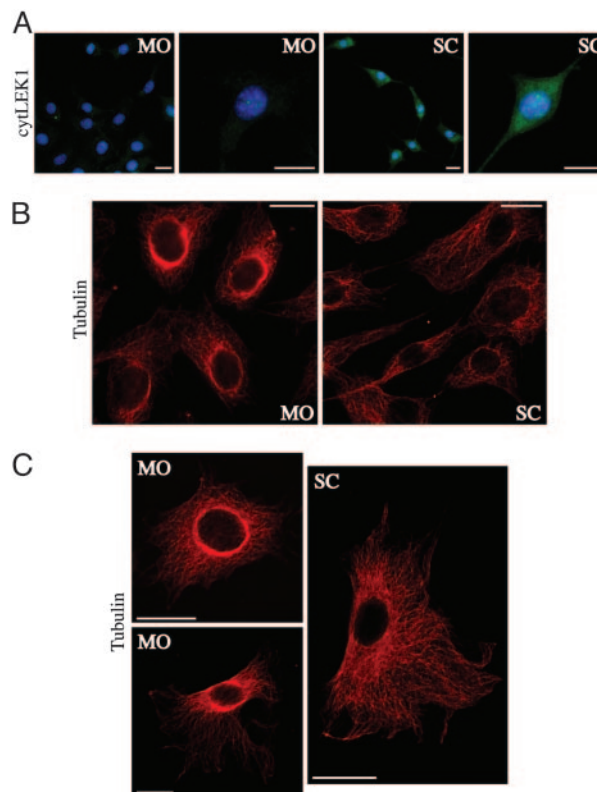


Fig. 7. LEK1 knockdown alters microtubule network organization. 3T3 cells were treated with LEK1-specific (MO) or standard control (SC) morpholinos and examined 72 h after treatment. (A) LEK1-specific morpholino-treated cells show a substantial but not complete knockdown of cytLEK1 protein (green), compared with controls. (B and C) The microtubule network (red) of LEK1-specific morpholino-treated cells is tightly focused around the nucleus when compared with control cells. DAPI (blue) was used to visualize nuclei. (Bars: A, 20 μ m; B and C, 10 μ m.)

bind NudE, did not lead to any changes in microtubule repolymerization after nocodazole treatment and washout (Fig. 6C). Note that both transfected and surrounding cells have microtubule networks emanating from organizing centers. Taken together, these experiments demonstrate that the presence of the NudE-binding domain of cytLEK1 causes nearly complete inhibition of microtubule repolymerization and may explain the intense effects on cell morphology and cytoskeleton that occur with its expression.

LEK1 Knockdown Alters Microtubule Network Organization. To further confirm the role of cytLEK1 in the LIS1 pathway, we examined the effects of knockdown of the LEK1 protein by using morpholino antisense oligomers. These LEK1 morpholinos had previously been confirmed to effectively and specifically knock down LEK1 protein expression (24). We verified that cytLEK1 protein expression is indeed knocked down by LEK1 morpholino versus standard control morpholino treatment in 3T3 fibroblasts (Fig. 7A). Whereas control-treated cells displayed a uniform distribution of microtubules throughout the cytoplasm, LEK1 knockdown resulted in a tight perinuclear focusing of microtubules (Fig. 7B and C), similar but less severe than that observed with expression of myc-C and representative of disruption of microtubule transport to the cell periphery. Because the LIS1 pathway is critical for this transport process, inhibition of the function of any member of the LIS1 pathway has consistently resulted in accumulation of microtubules around the nucleus (6, 30, 31). This result thus provides additional evidence that cytLEK1 expression is critical for LIS1 pathway function.

Discussion

In the present study, we demonstrate that cytLEK1 is a member of the LIS1 pathway. Our biochemical analyses localized the NudE-binding domain in cytLEK1 to an 80-aa region adjacent to the spectrin repeat. This C domain is critical for interaction with NudE and efficiently colocalizes with endogenous NudE near the centrosome. Importantly, this NudE-binding domain specifically confers resistance to detergent treatment; thus, it may assist binding of cytLEK1 to the cytoskeleton and mediate its molecular effects. Computer analysis of the C domain predicts a coiled-coil conformation but does not reveal any other known protein motifs (35, 36). Additionally, identification of the cytLEK1-binding region in NudE reveals a partial overlap with the NudE(L) dynein-binding domain (10), thus demonstrating the potential for molecular regulation of microtubule function by means of protein-protein interactions in these regions.

Alteration of cytLEK1 function was predicted to perturb specific functions of the LIS1 pathway. We postulated that isolation of the C domain from any other functional domains present in intact cytLEK1 would produce a dominant negative effect, and, indeed, this appears to be the case. The most prominent phenotype resulting from expression of myc-C is a drastic collapse of the cytoskeletal network accompanied by a severe change in cell shape. Importantly, a similar phenotype is also observed in cells in which LEK1 is knocked down with morpholinos but not in cells expressing full-length cytLEK1 or myc-N+R. The less severe phenotype in LEK1 knockdown cells is likely due to the presence of residual cytLEK1 remaining after morpholino treatment or simple variation between the two methods of disruption. Nonetheless, the critical role of cytLEK1 in microtubule network organization is evident in both experimental models. Additionally, cytLEK1 dysfunction alters the distribution of endogenous LIS1 pathway members, which appear to be decreased at the cell periphery and trapped near the nucleus with myc-C. Because this change is evident even before cells exhibit a rounded morphology, the dominant negative effect of myc-C on microtubule function is partially due to disrupting the movement and localization of these proteins. The tight perinuclear distribution of microtubules observed here with cytLEK1 dysfunction has previously been detected in *LIS1* heterozygous fibroblasts and in dynein and Nudel dysfunction studies and is attributed to the role of the LIS1 pathway in dynein-directed outward movement of microtubules (6, 30, 31). Studies using a dominant negative LIS1 protein have also revealed abnormalities in cell shape (14). In addition to disrupting existing microtubule networks, expression of myc-C also results in a nearly complete inability to repolymerize

microtubule networks after nocodazole challenge. Similarly, LIS1, dynein, and Nudel misexpression alter microtubule polymerization and localization after nocodazole treatment (6, 30). Overexpression of GFP-mNudE results in the formation of additional microtubule-organizing centers in the cell and disrupts normal microtubule organization (8). Finally, dysfunction of the LIS1 pathway, as with cytLEK1, alters the localization of pathway members (6, 7, 9, 10). Thus, all our results are consistent with previously reported experiments on LIS1 pathway members and validate a role for cytLEK1 in this pathway. Furthermore, we have never observed a mitotic figure in our limited number of myc-C-expressing cells, and our laboratory has shown previously that LEK1 depletion results in disruption of proliferation and increase in apoptosis (24). Similarly, Nudel depletion results in rapid apoptosis of cells (13), whereas loss of LIS1 or NudE causes proliferation defects (5, 7, 12). Thus, altering the function of cytLEK1 or LIS1 pathway members results in similar cellular perturbations and phenotypes, which supports our hypothesis that cytLEK1 is a member of the LIS1 pathway.

The present biochemical, cytological, and functional data suggest that cytLEK1 has the potential to play a broad role in the LIS1 pathway. First, because the dominant negative myc-C protein, which binds NudE, drastically inhibits microtubule repolymerization after nocodazole challenge, cytLEK1 likely has an important function at the centrosome. We also postulate that NudE plays a role in this cytoskeletal process through its interaction with cytLEK1, consistent with the known function of NudE as an ectopic microtubule-organizing center in cells (8). The currently unclear role of noncentrosomally located NudE (Figs. 3 and 4) (8–11) may also be regulated by cytLEK1, which is broadly distributed in the cytoplasm. Furthermore, the strong colocalization of cytLEK1 with LIS1 pathway members near the nucleus and its function in microtubule transport suggest that cytLEK1 may participate in additional dynein-directed movements of organelles and vesicles (6, 13). In summary, cytLEK1 likely influences important cellular processes regulated by the LIS1 pathway, including proliferation and migration (12, 37). Whether cytLEK1 serves simply as a scaffold or has a more active role in these pathway functions remains to be elucidated. Future binding studies to reveal additional interaction partners of cytLEK1 and generation of a *LEK1* conditional knockout mouse will help determine its function in regulating the LIS1 pathway during embryonic development.

We thank L. Smith, B. Robertson, K. Price, S. Hanks, and members of the D.M.B. laboratory for assistance. This work was supported by National Institutes of Health Grant HL37675 (to D.M.B.) and National Institutes of Health Fellowship HL07411 (to V.S.).

- Hirokawa, N. (1998) *Science* **279**, 519–526.
- Gibbons, I. R. (1996) *Cell Struct. Funct.* **21**, 331–342.
- Banks, J. D. & Heald, R. (2001) *Curr. Biol.* **11**, R128–R131.
- Hirotsune, S., Fleck, M. W., Gambello, M. J., Bix, G. J., Chen, A., Clark, G. D., Ledbetter, D. H., McBain, C. J. & Wynshaw-Boris, A. (1998) *Nat. Genet.* **19**, 333–339.
- Liu, Z., Steward, R. & Luo, L. (2000) *Nat. Cell Biol.* **2**, 776–783.
- Smith, D. S., Niethammer, M., Ayala, R., Zhou, Y., Gambello, M. J., Wynshaw-Boris, A. & Tsai, L. H. (2000) *Nat. Cell Biol.* **2**, 767–775.
- Faulkner, N. E., Dujardin, D. L., Tai, C. Y., Vaughan, K. T., O'Connell, C. B., Wang, Y. & Vallee, R. B. (2000) *Nat. Cell Biol.* **2**, 784–791.
- Feng, Y., Olson, E. C., Stukenberg, P. T., Flanagan, L. A., Kirschner, M. W. & Walsh, C. A. (2000) *Neuron* **28**, 665–679.
- Niethammer, M., Smith, D. S., Ayala, R., Peng, J., Ko, J., Lee, M. S., Morabito, M. & Tsai, L. H. (2000) *Neuron* **28**, 697–711.
- Sasaki, S., Shionoya, A., Ishida, M., Gambello, M. J., Yingling, J., Wynshaw-Boris, A. & Hirotsune, S. (2000) *Neuron* **28**, 681–696.
- Yan, X., Li, F., Liang, Y., Shen, Y., Zhao, X., Huang, Q. & Zhu, X. (2003) *Mol. Cell Biol.* **23**, 1239–1250.
- Feng, Y. & Walsh, C. A. (2004) *Neuron* **44**, 279–293.
- Liang, Y., Yu, W., Li, Y., Yang, Z., Yan, X., Huang, Q. & Zhu, X. (2004) *J. Cell Biol.* **164**, 557–566.
- Cahana, A., Escamez, T., Nowakowski, R. S., Hayes, N. L., Giacobini, M., von Holst, A., Shmueli, O., Sapir, T., McConnell, S. K., Wurst, W., et al. (2001) *Proc. Natl. Acad. Sci. USA* **98**, 6429–6434.
- Shmueli, O. & Reiner, O. (2000) *Dev. Genes Evol.* **210**, 51–54.
- Wei, Y., Bader, D. & Litvin, J. (1996) *Development (Cambridge, U.K.)* **122**, 2779–2789.
- Zhu, X., Mancini, M. A., Chang, K. H., Liu, C. Y., Chen, C. F., Shan, B., Jones, D., Yang-Feng, T. L. & Lee, W. H. (1995) *Mol. Cell Biol.* **15**, 5017–5029.
- Pabon-Pena, L. M., Goodwin, R. L., Cise, L. J. & Bader, D. (2000) *J. Biol. Chem.* **275**, 21453–21459.
- Liao, H., Winkfein, R. J., Mack, G., Rattner, J. B. & Yen, T. J. (1995) *J. Cell Biol.* **130**, 507–518.
- Goodwin, R. L., Pabon-Pena, L. M., Foster, G. C. & Bader, D. (1999) *J. Biol. Chem.* **274**, 18597–18604.
- Zhu, X. (1999) *Mol. Cell Biol.* **19**, 1016–1024.
- Redkar, A., deRiel, J. K., Xu, Y. S., Montgomery, M., Patwardhan, V. & Litvin, J. (2002) *Gene* **282**, 53–64.
- Zhu, X., Chang, K. H., He, D., Mancini, M. A., Brinkley, W. R. & Lee, W. H. (1995) *J. Biol. Chem.* **270**, 19545–19550.
- Ashe, M., Pabon-Pena, L., Dees, E., Price, K. L. & Bader, D. (2004) *J. Biol. Chem.* **279**, 664–676.
- Djinovic-Carugo, K., Gautel, M., Ylanne, J. & Young, P. (2002) *FEBS Lett.* **513**, 119–123.
- O'Shea, E. K., Rutkowski, R., Stafford, W. F., III, & Kim, P. S. (1989) *Science* **245**, 646–648.
- Reiner, O., Bar-Am, I., Sapir, T., Shmueli, O., Carrozzo, R., Lindsay, E. A., Baldini, A., Ledbetter, D. H. & Cahana, A. (1995) *Genomics* **30**, 251–256.
- Altschul, S. F., Gish, W., Miller, W., Myers, E. W. & Lipman, D. J. (1990) *J. Mol. Biol.* **215**, 403–410.
- Vallee, R. B., Tai, C. & Faulkner, N. E. (2001) *Trends Cell Biol.* **11**, 155–160.
- Shu, T., Ayala, R., Nguyen, M. D., Xie, Z., Gleeson, J. G. & Tsai, L. H. (2004) *Neuron* **44**, 263–277.
- Ahmad, F. J., Echeverri, C. J., Vallee, R. B. & Baas, P. W. (1998) *J. Cell Biol.* **140**, 391–401.
- Sapir, T., Elbaum, M. & Reiner, O. (1997) *EMBO J.* **16**, 6977–6984.
- Toomre, D., Keller, P., White, J., Olivo, J. C. & Simons, K. (1999) *J. Cell Sci.* **112**, 21–33.
- Giodini, A., Kallio, M. J., Wall, N. R., Gorbisky, G. J., Tognin, S., Marchisio, P. C., Symons, M. & Altieri, D. C. (2002) *Cancer Res.* **62**, 2462–2467.
- Lupas, A., Van Dyke, M. & Stock, J. (1991) *Science* **252**, 1162–1164.
- Falquet, L., Pagni, M., Bucher, P., Hulo, N., Sigrist, C. J., Hofmann, K. & Bairoch, A. (2002) *Nucleic Acids Res.* **30**, 235–238.
- Dujardin, D. L., Barnhart, L. E., Stehman, S. A., Gomes, E. R., Gundersen, G. G. & Vallee, R. B. (2003) *J. Cell Biol.* **163**, 1205–1211.